Summary of the 2019/2020 Asian Winter Monsoon

This report summarizes the characteristics of the surface climate and atmospheric/oceanographic considerations related to the Asian winter monsoon for 2019/2020.

Note: The Japanese 55-year Reanalysis (JRA-55; Kobayashi et al. 2015) atmospheric circulation data and COBE-SST (Ishii et al. 2005) sea surface temperature (SST) data were used for this investigation. NOAA Interpolated Outgoing Longwave Radiation (OLR) data (Liebmann and Smith 1996) provided by the U.S. NOAA Earth System Research Laboratory (ESRL) from their web site at https://www.esrl.noaa.gov/psd/ was referenced to infer tropical convective activity. The base period for the normal is 1981 to 2010. The term "anomaly" as used in this report refers to deviation from the normal.

1. Surface climate conditions

Temperatures for December 2019 to February 2020 (Figure 5-1) were above normal in many parts of Asia and Siberia, with the exception of the area from central China to the northern part of South Asia. In particular, very warm conditions continued throughout the period from eastern Japan to southeastern China and in the southern part of South Asia. Seasonal mean temperatures in Japan, Korea and Russia were the highest for winter since 1897/1898 (Japan Meteorological Agency), 1972/1973 (Korea Meteorological Administration) and 1890/1891 (Hydrometcenter of Russia), respectively.

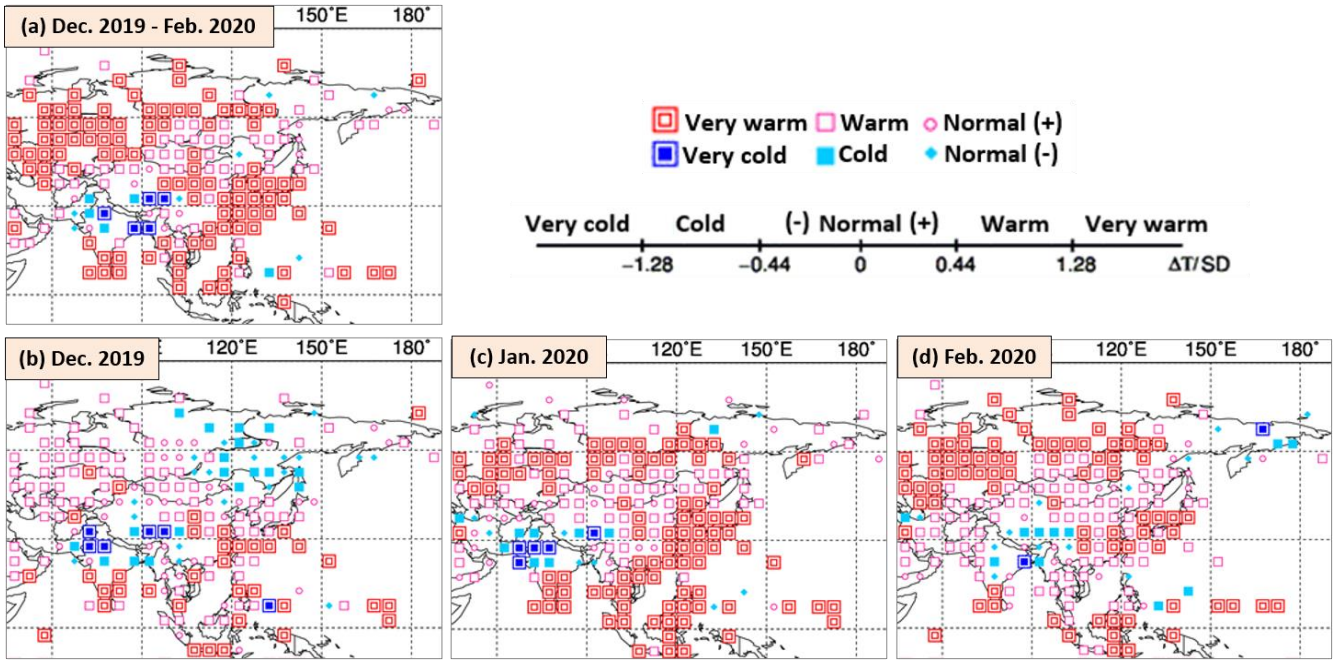

Figure 5-1 (a) Three-month mean temperature anomalies for December 2019 to February 2020, and monthly mean temperature anomalies for (b) December 2019, (c) January 2020 and (d) February 2020

Categories are defined by the three-month/monthly mean temperature anomaly against the normal divided by its standard deviation and averaged in 5° × 5° grid boxes. The thresholds of each category are -1.28, -0.44, 0, +0.44 and +1.28. Standard deviations were calculated from 1981- 2010 statistics. Areas over land without graphical marks are those where observation data are insufficient or where normal data are unavailable.

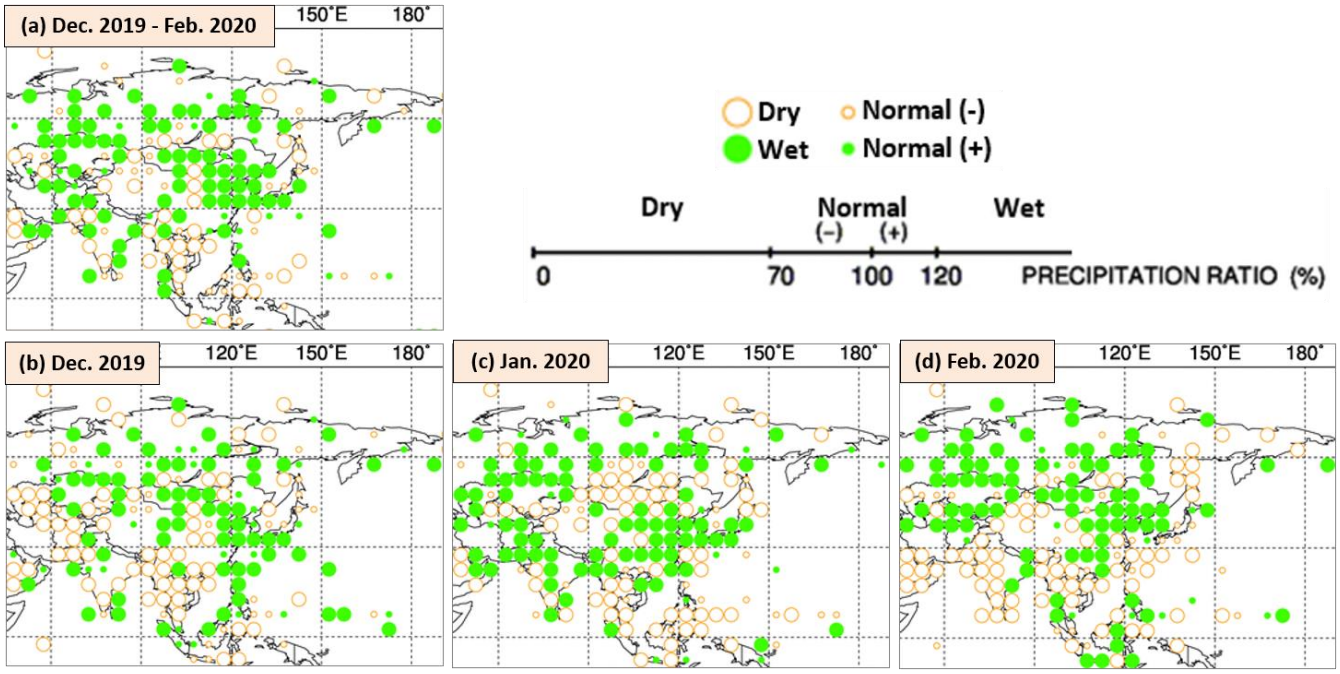

Figure 5-2 (a) Three-month precipitation ratio for December 2019 to February 2020, and monthly precipitation ratio for (b) December 2019, (c) January 2020 and (d) February 2020

Categories are defined by the three-month/monthly precipitation ratio against the normal and averaged in 5° × 5° grid boxes. The thresholds of each category are 70, 100 and 120%. Areas over land without graphical marks are those where observation data are insufficient or where normal data are unavailable.

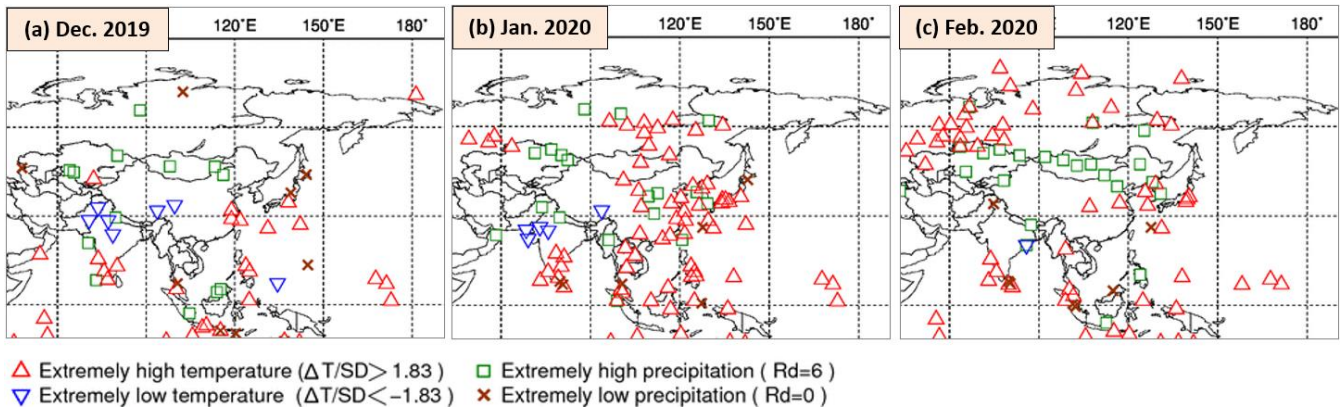

Figure 5-3 Extreme climate stations for (a) December 2019, (b) January 2020 and (c) February 2020

ΔT, SD and Rd indicate temperature anomaly, standard deviation and quintile, respectively.

Precipitation amounts during this period (Figure 5-2) were above normal in the eastern part of East Asia, from the western part of Eastern Siberia to Central Siberia, and in and around Central Asia, and were below normal in the northern part of Southeast Asia.

Figure 5-3 shows extreme climate conditions observed between December 2019 and February 2020. In December, extremely high temperatures were seen in southern India and the southern part of Southeast Asia, and extremely low temperatures were seen from northeastern Pakistan to central India. In January, extremely high temperatures

were seen in and around the central part of Central Siberia, from eastern to central East Asia, in Southeast Asia, and from southern India to Sri Lanka, while extremely low temperatures were seen from western India to southern Pakistan. Extremely high precipitation amounts were observed in northeastern Kazakhstan. In February, extremely high temperatures were seen from the northwestern part of Eastern Siberia to the northern part of Western Siberia, from the central part of Western Siberia to the northwestern part of Central Asia, from eastern Japan to central China, from southwestern India to Sri Lanka, and in the southern part of Southeast Asia. Extremely high precipitation amounts were observed from northeastern China to the central part of Central Asia.

2. Characteristic atmospheric circulation and oceanographic conditions

2.1 Conditions in the tropics

In the equatorial Pacific, remarkably positive SST anomalies were observed in the western part. In the North Pacific, remarkably positive SST anomalies were observed from east of the Philippines to far east of Japan and in central and eastern tropical regions. In the Indian Ocean, remarkably positive SST anomalies were observed across almost the entire tropical region (Figure 5-4).

Convective activity inferred from OLR during this period (Figure 5-5) was persistently enhanced over the western tropical Indian Ocean and around the date line in the equatorial Pacific, reflecting higher-than-normal SSTs in these regions, and was suppressed over the Maritime Continent.

In the upper troposphere, large-scale divergent anomalies were seen over the western Indian Ocean and around the date line in association with enhanced convective activity, and convergent anomalies were observed over the Maritime Continent (Figure 5-6 (a)). In the 200-hPa stream function field (Figure 5-6 (b)), a wave train was seen from Europe to Japan along the subtropical jet stream, with anti-cyclonic circulation anomalies over the Arabian Sea and Japan, and cyclonic circulation anomalies over southern China. This meandering of the jet stream was associated with enhanced convection over the western Indian Ocean and suppressed convection over the Maritime Continent, and partly originated from the northward meandering of the westerly jet stream over Europe. In the lower troposphere (Figure 5-6 (c)), anti-cyclonic circulation anomalies straddling the equator were seen from the central tropical Indian Ocean to the Maritime Continent in association with suppressed convection over the Maritime Continent, and cyclonic circulation anomalies straddling the equator were seen west of the date line in the tropical Pacific.

The active phase of equatorial intraseasonal oscillation propagated eastward globally during winter 2019/2020, overlapping with persistently enhanced convective activity over the western Indian Ocean and around the date line (Figure 5-7).

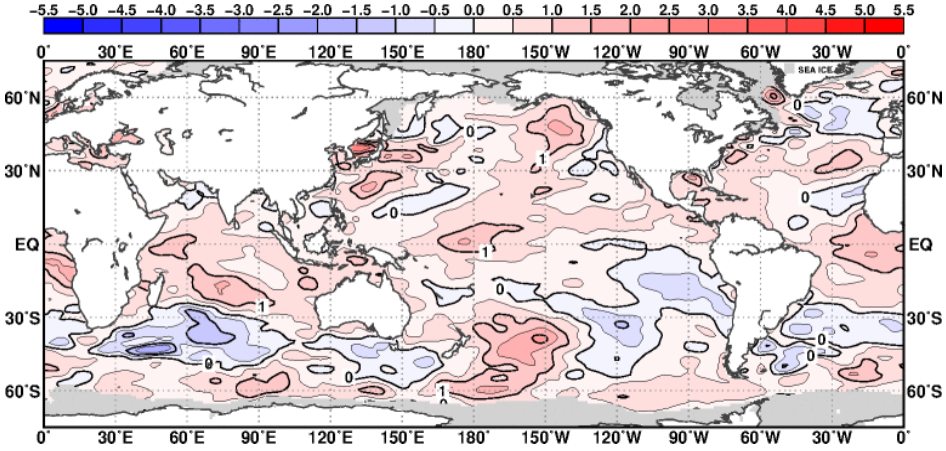

Figure 5-4 Three-month mean sea surface temperature (SST) anomalies [°C] for December 2019 to February 2020

The contour interval is 0.5°C.

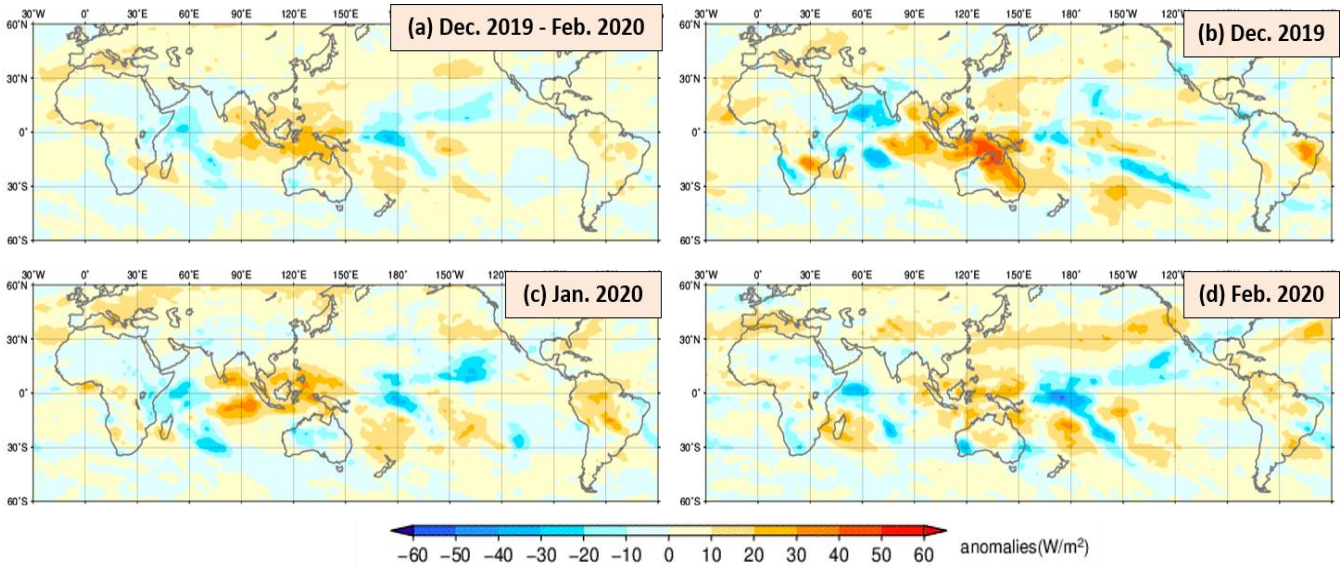

Figure 5-5 Outgoing longwave radiation (OLR) anomalies [W/m^2] for (a) December 2019 to February 2020, (b) December 2019, (c) January 2020 and (d) February 2020

The blue and red shading indicates areas of enhanced and suppressed convective activity, respectively.

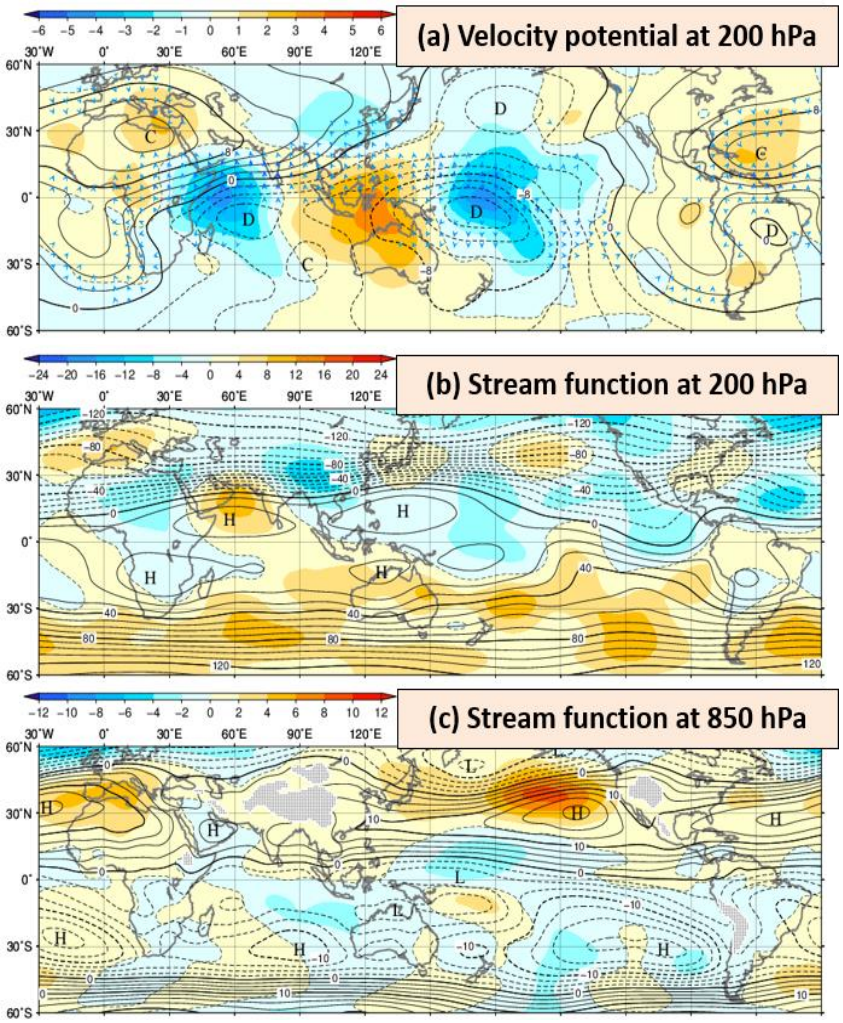

Figure 5-6 Three-month mean (a) 200-hPa velocity potential, (b) 200-hPa stream function and (c) 850-hPa stream function for December 2019 to February 2020 [unit: 10^6 m^2/s]

(a) The contours indicate velocity potential at intervals of 2 × 10^6 m^2/s, and the shading shows velocity potential anomalies. D and C indicate the bottom and the peak of velocity potential, corresponding to the centers of large-scale divergence and convergence, respectively. The vectors show divergent wind. (b, c) The contours indicate stream function at intervals of (b) 10 × 10^6 m^2/s and (c) 2.5 × 10^6 m^2/s, and the shading shows stream function anomalies. H and L denote the centers of anti-cyclonic and cyclonic circulations, respectively.

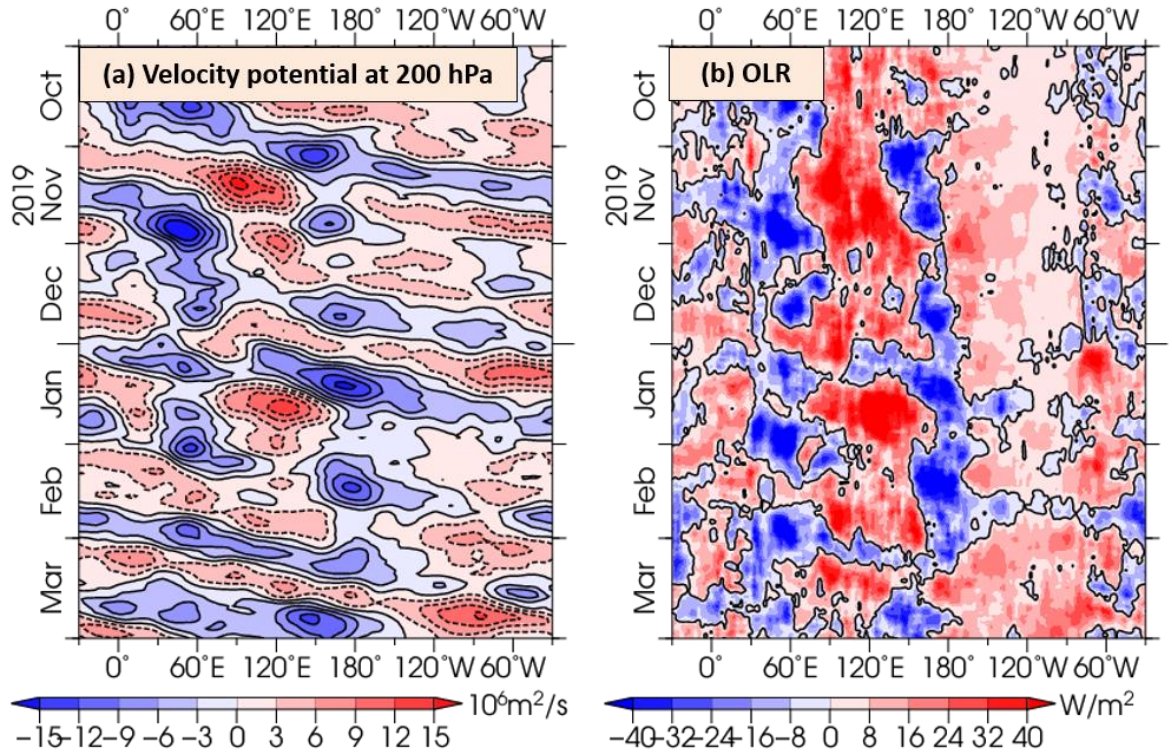

Figure 5-7 Time-longitude cross section of seven-day running mean (a) 200-hPa velocity potential anomalies [10^6 m^2/s] and (b) outgoing longwave radiation (OLR) anomalies [W/m^2] around the equator (5°S – 5°N) for October 2019 to March 2020

(a) The blue and red shading indicates areas of divergence and convergence anomalies, respectively. (b) The blue and red shading indicates areas of enhanced and suppressed convective activity, respectively.

2.2 Conditions in the extratropics

In the 500-hPa height field during winter 2019/2020 (Figure 5-8), positive anomalies were seen over Japan, the mid-latitudes in the central and eastern North Pacific, and southern Europe, while negative anomalies were seen over Alaska and near Iceland. As shown in Figure 5-9, the positive phase of the Arctic Oscillation (AO; also known as the Northern Annular Mode) with negative anomalies over the northern polar region and positive anomalies over the Northern Hemisphere mid-latitudes was dominant in January and February. The Aleutian Low and the Siberian High were weaker than normal during winter 2019/2020, indicating a weaker-than-normal East Asian Winter Monsoon that contributed to the extremely warm conditions observed in East Asia.

The polar front jet stream was clearly seen over northern Eurasia in association with the positive AO, which is linked with weak cold-air mass accumulation over a broad area from Europe to Siberia. The subtropical jet stream shifted southward of its normal position from the northern part of South Asia to southern China and meandered northward over the mid-latitudes in the western North Pacific (Figure 5-10 (a)). These conditions contributed to weaker-than-normal cold-air flow over East Asia. Temperatures at 850 hPa were above normal from Europe via Central Siberia to Japan, and below normal over the northern part of South Asia (Figure 5-10 (b)).

(SATO Hitoshi, Tokyo Climate Center)

References

Ishii, M., A. Shouji, S. Sugimoto and T. Matsumoto, 2005: Objective analyses of sea-surface temperature and marine meteorological variables for the 20th century using ICOADS and the Kobe Collection. *Int. J. Climatol.*, **25**, 865-879.

Kobayashi, S., Y. Ota, Y. Harada, A. Ebita, M. Moriya, H. Onoda, K. Onogi, H. Kamahori, C. Kobayashi, H. Endo, K. Miyaoka, and K. Takahashi, 2015: The JRA-55 Reanalysis: General specifications and basic characteristics. *J. Meteor. Soc. Japan*, **93**, 5 – 48.

Liebmann, B., and C. A. Smith, 1996: Description of a complete (interpolated) outgoing longwave radiation dataset. *Bull. Amer. Meteor. Soc.*, **77**, 1275–1277.

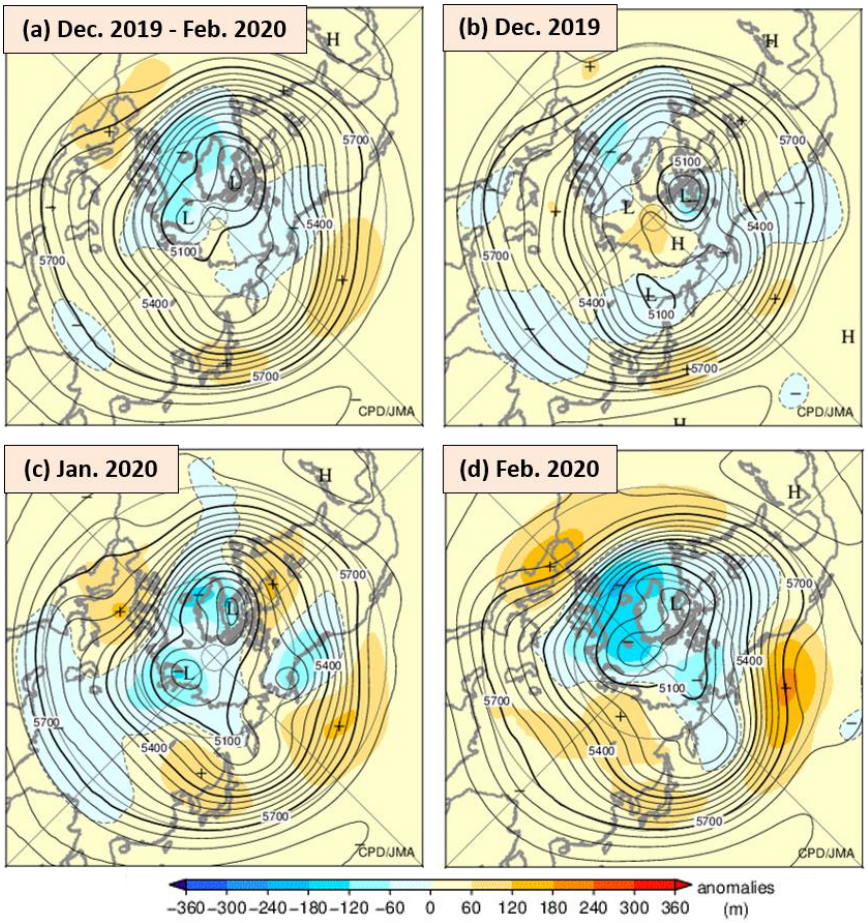

Figure 5-8 500-hPa height [m] for (a) December 2019 to February 2020, (b) December 2019, (c) January 2020 and (d) February 2020

The contours indicate height at intervals of 60 m, and the shading denotes height anomalies. H and L indicate the peak and bottom of 500-hPa height, respectively, and + (plus) and – (minus) show the peak and bottom of anomalies, respectively.

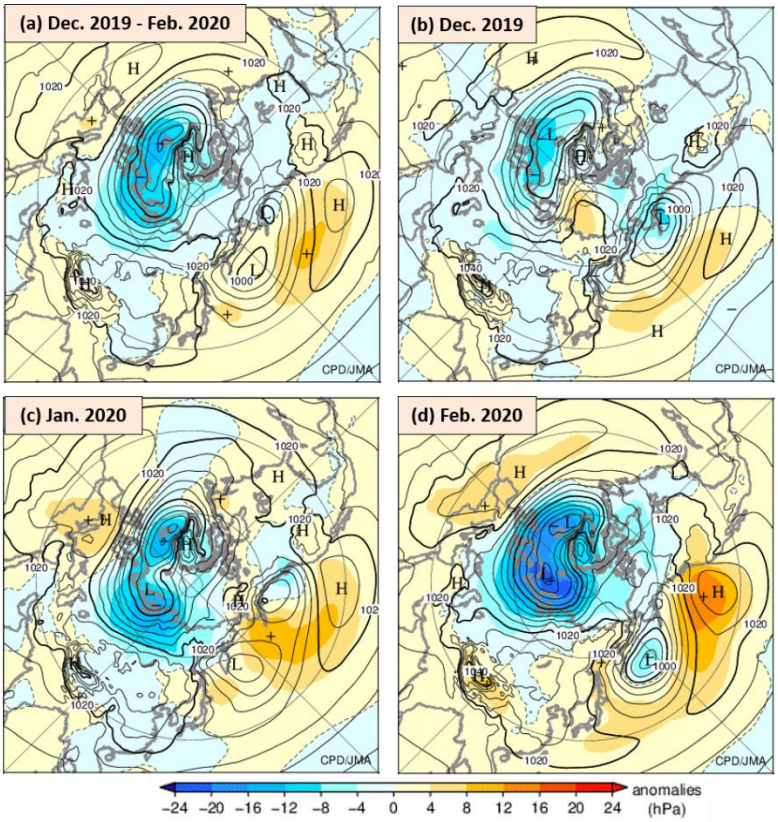

Figure 5-9 Sea level pressure [hPa] for (a) December 2019 to February 2020, (b) December 2019, (c) January 2020 and (d) February 2020

The contours indicate sea level pressure at intervals of 4 hPa, and the shading shows related anomalies. H and L indicate the centers of high and low pressure systems, respectively, and + (plus) and – (minus) show the peak and bottom of sea level pressure anomalies, respectively.

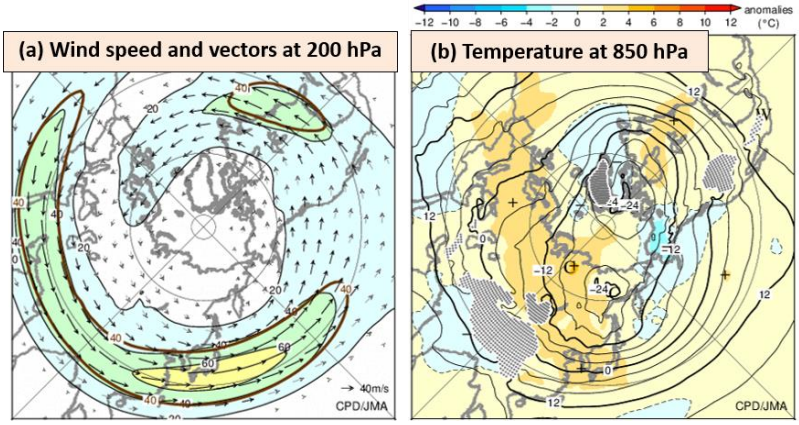

Figure 5-10 Three-month mean (a) 200-hPa wind speed and vectors [m/s] and (b) 850-hPa temperature [°C] for December 2019 to February 2020

(a) The black lines show wind speed at intervals of 20 m/s and the brown lines show its normal at intervals of 40 m/s. (b) The contours indicate temperature at intervals of 4 °C and the shading shows related anomalies.

<<Table of contents <Top of this article